

Mathematical Modeling of Solidification Paths in Ternary Alloys: Limiting Cases of Solute Redistribution

J.N. DuPONT

A simple mathematical framework is provided for calculating solidification paths of ternary alloys for equilibrium, paraequilibrium, and nonequilibrium conditions. The results are useful for estimating the possible range of primary solidification paths, the type of monovariant reaction expected to occur, and the relative amount of primary, monovariant eutectic and ternary eutectic constituents that form during solidification. Example calculations show that, for solidification of a ternary eutectic alloy under equilibrium conditions, the monovariant eutectic reaction will only occur when the nominal alloy concentration is above the maximum solid solubility. This result is similar to the binary case. For paraequilibrium conditions, a monovariant eutectic reaction is always expected to occur, but solidification can terminate before the invariant ternary eutectic reaction is reached. Finally, for nonequilibrium conditions, both the monovariant and invariant ternary eutectic reactions are always expected to occur, which is similar to the binary nonequilibrium case. The direction of liquid enrichment on the monovariant eutectic line can also be determined from the results.

I. INTRODUCTION

A. Binary Solidification

SOLIDIFICATION processing is used in a variety of fabrication methods such as casting, welding, laser surface treatment, and crystal growth. In many cases, products prepared from these processes are used in the as-solidified condition. In such applications, the mechanical properties and corrosion performance of the component are strongly influenced by the distribution of alloying elements and relative fraction of secondary constituents that form during the solidification process. Thus, it is often useful to make quantitative estimates of the resultant solidification microstructure as a means for controlling the ultimate component performance. Many models have been developed in the solidification literature on solute redistribution and microstructural development in binary alloys that are capable of accounting for factors such as dendrite tip undercooling, coarsening, and back diffusion, and several review articles have been published on the subject.^[1-4] While these models are quite useful, it is worth noting that most all conditions of solute redistribution in binary alloys must fall within two very simple cases: the lever law and so-called nonequilibrium Scheil equation.^[5] The first condition assumes that solute diffusion is infinitely fast in both the liquid and solid phases, equilibrium is maintained at the solid/liquid interface, and there is no undercooling during nucleation or growth. The latter condition invokes the same assumptions, except that solute diffusion is negligible in the solid.

The relation between liquid composition and fraction liquid for equilibrium solidification is given simply by

$$C_L = \frac{C_o}{(1-k)f_L + k} \quad [1]$$

where C_L is the liquid composition at any value of fraction liquid, f_L ; C_o is the nominal alloy composition; and k is the equilibrium distribution coefficient, defined as the ratio of solid to liquid compositions and assumed constant in Eq. [1]. The corresponding relation between C_L and f_L for the Scheil condition is given by

$$C_L = C_o f_L^{(k-1)} \quad [2]$$

These two limiting cases of solute redistribution in binary alloys are quite useful as they allow the possible ranges of microstructural development to be easily bound.

As an example, consider a binary eutectic A-B system shown in Figure 1, which exhibits linear solidus and liquidus lines, a k value (for solute element B) of 0.2, and a eutectic composition of 20 wt pct B. Figure 2 shows the variation in liquid composition during solidification under equilibrium (Eq. [1]) and nonequilibrium (Eq. [2]) conditions for two alloys: one below the maximum solid solubility with $C_o = 2$ wt pct B (Figure 2(a)) and one above the maximum solid solubility with $C_o = 5$ wt pct B (Figure 2(b)). For the 2 wt pct B alloy, the solidification conditions under each extreme are quite different. Under equilibrium conditions, the liquid composition never becomes enriched to the eutectic composition because solute in the solid is uniformly distributed and therefore capable of dissolving all the solute before the eutectic point is reached in the liquid. Note from Eq. [1] that the maximum solute enrichment in the liquid for the equilibrium condition is given as C_o/k , which occurs when $f_L = 0$. In this case, $C_o/k < C_e$ (the eutectic composition). The resultant microstructure directly after solidification would simply consist of primary α with a uniform distribution of B. For the nonequilibrium case, Eq. [2] suggests that $C_L \rightarrow \infty$ as $f_L \rightarrow 0$ (for $k < 1$), which indicates the liquid composition will always become enriched to the eutectic point. This can be attributed to the lack of diffusion in the primary α phase, which leads to the inability of all the solute to be incorporated into the primary phase. Thus, directly below the eutectic temperature, the 2 wt pct B alloy exhibits primary α with a concentration

J.N. DuPONT, Associate Professor, is with the Department of Materials Science & Engineering, Lehigh University, Bethlehem, PA 18015-3195. Contact e-mail: jnd1@lehigh.edu

Manuscript submitted October 7, 2005.

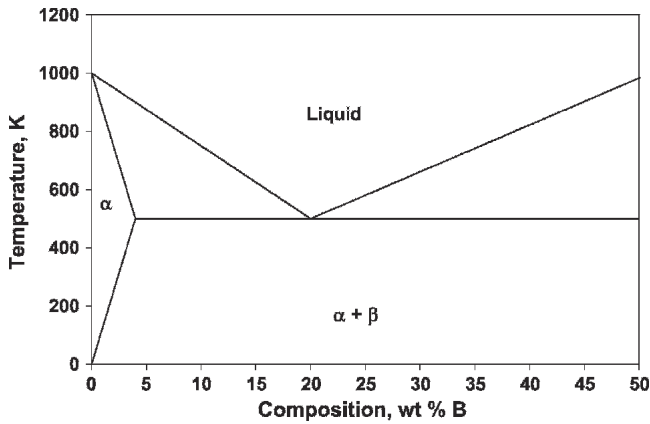
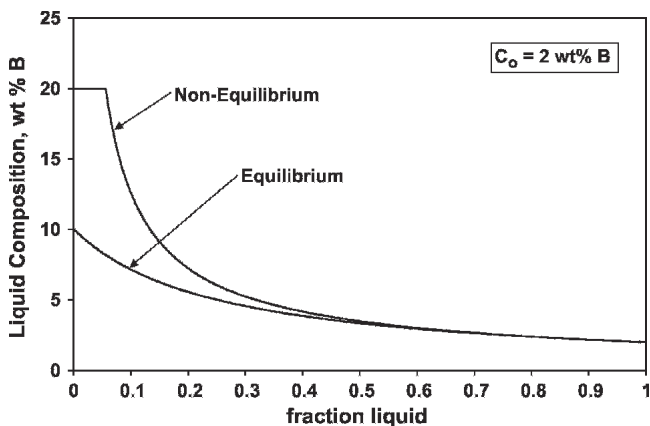
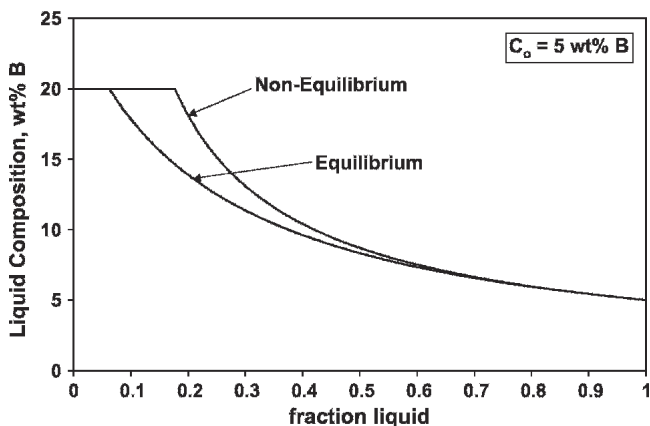


Fig. 1—A rich portion of a hypothetical A-B binary eutectic phase diagram.



(a)



(b)

Fig. 2—Variation in liquid composition with fraction liquid for equilibrium and nonequilibrium conditions for alloys with $C_o = 2$ wt pct (Figure 2(a)) and $C_o = 5$ wt pct B (Figure 2(b)).

gradient and 0.06 weight fraction of the α/β eutectic when solidified under nonequilibrium conditions.

The two extreme solute redistribution behaviors for the 5 wt pct B alloy are compared in Figure 2(b). For the equilibrium case, the liquid composition will become enriched to the eutectic point because the nominal composition is

above the maximum solid solubility. In other words, $C_o/k > C_e$. This eutectic reaction occurs when there is 0.06 weight fraction remaining liquid. Thus, the solidification microstructure directly after equilibrium solidification consists of primary α with a uniform distribution of B and 0.06 weight fraction of the α/β eutectic. For the nonequilibrium case, the liquid composition is always higher at any stage during solidification (*i.e.*, any particular value of f_L) because the solid does not dissolve as much solute. As a result, more liquid remains when the eutectic composition is reached (0.18 weight fraction) and more of the eutectic constituent forms in the solidification microstructure. The final alloy here exhibits primary α with a concentration gradient and 0.18 weight fraction of the α/β eutectic (three times the weight fraction of eutectic that formed for the equilibrium case).

B. Ternary Solidification

The solidification paths (*i.e.*, variation in liquid composition during solidification) in binary alloys are easy to understand because the phase diagram is planar and the liquid composition is therefore restricted to follow the liquidus line. Thus, the solidification path is easily interpreted by direct inspection of the binary diagram. However, with ternary alloys, the addition of a third element changes the planar phase diagram into a volume and the liquidus line transforms into a surface. Here, the solidification path and resultant solidification microstructure cannot be determined by direct inspection of the liquidus surface because the path will depend on the relative solute redistribution behavior of each solute in the system.^[6,7]

As an example, Figure 3 schematically shows the C-rich corner of the liquidus surface for an A-B-C ternary eutectic system that exhibits three primary solidification phases: α , β , and γ . An alloy with a nominal composition located in the C-rich corner could potentially exhibit six different solidification paths. In Figure 3(a), the liquid composition is never enriched to either the α/β or α/γ monovariant eutectic line. The microstructure developed under this solidification path would simply consist of primary α . This is similar to equilibrium solidification of a binary alloy, which has a nominal composition below the maximum solid solubility. In Figures 3(b) and (c), the liquid composition is enriched to the point where the primary solidification path intersects the monovariant eutectic line separating the α and β phases. The solidification path then follows the eutectic line as the α and β phases form simultaneously from the liquid by a monovariant eutectic reaction. Depending on the diffusivity of A and B in the solid,^[7] solidification could be completed along the eutectic line (Figure 3(b)) or the liquid composition could be enriched all the way to the ternary eutectic composition (Figure 3(c)), at which point the ternary $\alpha/\beta/\gamma$ eutectic constituent will form isothermally. For the case shown in Figure 3(b), the microstructure will contain the α primary phase and the binary-type α/β eutectic constituent. The microstructure formed from the solidification path shown in Figure 3(c) will exhibit primary α , the eutectic-type α/β constituent, and the $\alpha/\beta/\gamma$ ternary eutectic.

In Figures 3(d) and (e), the primary solidification path is oriented such that it intersects the α/γ monovariant eutectic

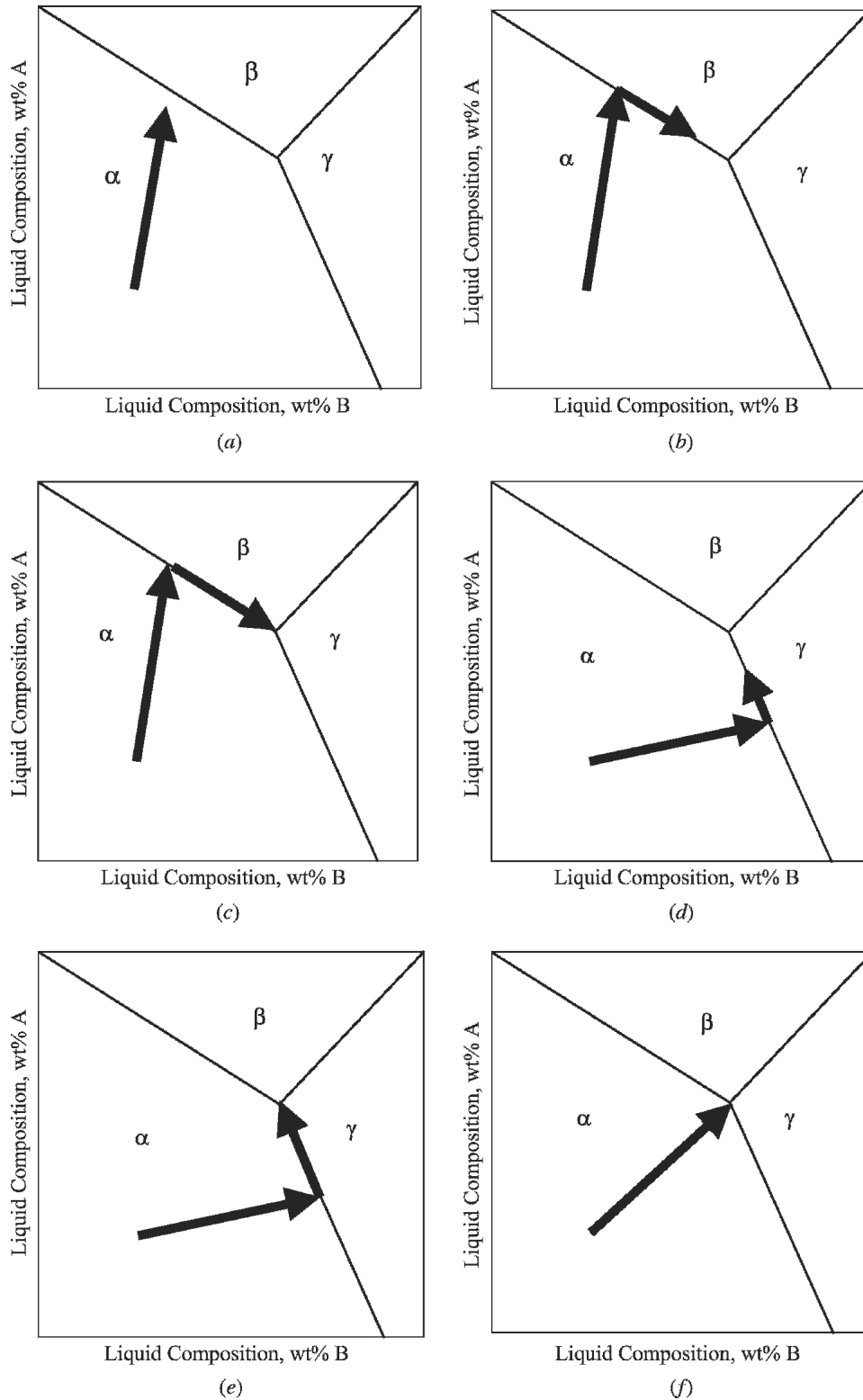


Fig. 3—C-rich corner of an A-B-C ternary eutectic liquidus surface demonstrating possible solidification paths.

line instead of the α/β line. This could occur if the diffusivity of B in α is very low (relative to element A) or the solubility of B in α is low (*i.e.*, low k), which would cause the liquid to become highly enriched in B during solidification. The solidification path will then follow the mono-

variant eutectic line as the α and γ phases form simultaneously from the liquid by a monovariant eutectic reaction. Depending on the diffusivity of A and B in the solid, solidification could be completed along the α/γ eutectic line (Figure 3(d)), or the liquid composition could

be enriched all the way to the ternary eutectic (Figure 3(e)) at which point the ternary $\alpha/\beta/\gamma$ eutectic constituent will form isothermally. For the case shown in Figure 3(d), the microstructure will contain the α primary phase and the binary-type α/γ eutectic constituent. The microstructure formed from the solidification path shown in Figure 3(e) will exhibit primary α , the eutectic-type α/γ constituent, and the $\alpha/\beta/\gamma$ ternary eutectic. Finally, Figure 3(f) demonstrates the case in which the primary solidification path directly intersects the $\alpha/\beta/\gamma$ ternary eutectic point. In this case, the as-solidified microstructure would exhibit primary α and the ternary $\alpha/\beta/\gamma$ ternary eutectic constituent.

The preceding examples illustrate the difficulty in making simple quantitative estimates of solidification paths and resultant microstructures in ternary alloys. Although it is not typically recognized, relatively simple solidification path equations can be derived for limiting cases of solute redistribution in ternary alloys. These equations, which are analogous to those already known and used for binary alloys, form a set of limiting conditions for making quantitative estimates of microstructural development in ternary alloys. Binary solidification contains two limiting cases that are essentially set by the diffusion behavior of the solute in the solid: (1) infinitely fast diffusion in the solid and (2) negligible diffusion in the solid. For ternary solidification, three limiting cases can be identified based on the diffusivity of solute in the solid phases: (1) negligible diffusion of each solute in the solid phases, referred to as nonequilibrium solidification; (2) negligible diffusion of one solute in the solid phases and infinitely fast diffusion of the other solute in the solid phases, referred to here as paraequilibrium; and (3) infinite diffusion of each solute in the solid phases (equilibrium). The objective of this article is to derive the solute redistribution equations for each of these conditions for both the primary and eutectic stages of solidification and to demonstrate the use of these equations for predicting solidification paths and resultant microstructures of ternary alloy systems.

It is recognized that similar information can often be obtained in newer computational software codes that permit variations in partition coefficients, solid and liquid diffusivities, and phase boundary positions during solidification. However, the procedure described here is still very useful because it provides a simple method for bounding the range of behaviors for more complicated conditions, similar to that of the equilibrium and nonequilibrium binary equations described previously. In addition, the approach presented here can often be combined with calculated phase diagram information and partition coefficients from software codes in order to evaluate the influence of each alloy parameter (*e.g.*, k values and phase boundary positions) on solidification behavior and resultant microstructure. This approach is often very useful for modeling multicomponent alloys in a straightforward manner using a ternary analog^[7] and for identifying sources of inaccuracies when results from software codes do not match experimental results.^[8]

II. SOLUTE REDISTRIBUTION EQUATIONS

For each condition considered here, two sets of solute redistribution equations will be developed. The first set describes the variation in liquid composition and fraction

liquid during the primary stage of solidification (*e.g.*, $L \rightarrow \alpha$ in Figure 3(a)). These expressions can be used to quickly identify if the liquid composition is enriched to a monovariant eutectic-type reaction and, if so, what type of reaction will occur (*i.e.*, $L \rightarrow (\alpha + \beta)$ or $L \rightarrow (\alpha + \gamma)$) and the weight fraction of total eutectic constituent that will form in the microstructure. The second set of expressions describes the variation in liquid composition and fraction liquid during the monovariant eutectic reaction. These expressions can be used to determine if the liquid composition is enriched to the isothermal ternary eutectic reaction (*e.g.*, $L \rightarrow \alpha + \beta + \gamma$) and the weight fractions of both the monovariant (*i.e.*, α/β or α/γ) and ternary eutectic ($\alpha/\beta/\gamma$) constituents.

A. Equilibrium Solidification

The assumptions for this condition are identical to those implemented for equilibrium binary solidification: infinite diffusion of each solute in the liquid and solid phases; equilibrium is maintained at the solid/liquid interface, and there is no undercooling during growth. Two additional assumptions are invoked here, namely, that the equilibrium distribution coefficient for each element in each phase is constant and that solute redistribution of each element occurs independently.

1. Primary $L \rightarrow \alpha$ solidification

The relation between fraction liquid and liquid composition for each solute (A and B) for this condition is

$$f_L = \frac{C_{oA} - k_{\alpha A} C_{LA}}{(1 - k_{\alpha A}) C_{LA}} \quad [3a]$$

$$f_L = \frac{C_{oB} - k_{\alpha B} C_{LB}}{(1 - k_{\alpha B}) C_{LB}} \quad [3b]$$

where f_L is the fraction liquid, C_{oj} is the nominal concentration of element j , C_{Lj} is the concentration of element j in the liquid, and k_{ij} is the equilibrium distribution coefficient for element j in phase i . An expression for the primary solidification path (*i.e.*, relation between C_{LA} and C_{LB}) can be obtained by setting expressions [3a] and [b] equal and solving for C_{LA}

$$C_{LA} = \frac{C_{oA}}{\left(\frac{1 - k_{\alpha A}}{1 - k_{\alpha B}}\right) \left(\frac{C_{oB} - k_{\alpha B} C_{LB}}{C_{LB}}\right) + k_{\alpha A}} \quad [4]$$

Equation [4] is the solidification path for primary $L \rightarrow \alpha$ solidification for equilibrium conditions and can be plotted directly on the liquidus surface. The plot is initiated at $C_{LA} = C_{oA}$ and $C_{LB} = C_{oB}$. If the value of $k_{\alpha B} < 1$, then solute is rejected from the solid to the liquid and C_{LB} will increase during solidification. In this case, the value of C_{LB} is repeatedly increased by some small amount ΔC_{LB} (*e.g.*, ~ 0.5 wt pct) and the corresponding value of C_{LA} is determined through Eq. [4] to trace out the primary solidification path. If the value of $k_{\alpha B} > 1$, then the solid becomes enriched in solute while the liquid becomes depleted in solute so that

C_{LB} will decrease during solidification. In this case, the value of C_{LB} is repeatedly reduced by some small amount ΔC_{LB} and the corresponding value of C_{LA} is determined through Eq. [4] to trace out the primary solidification path. The corresponding value of f_L at any liquid composition can be determined from Eq. [3a] or [b]. As demonstrated by example in Section III, the solidification path plot can be used to determine if a monovariant eutectic reaction will occur before all the liquid is consumed and, if so, what the reaction will be (*i.e.*, $L \rightarrow (\alpha + \beta)$ or $L \rightarrow (\alpha + \gamma)$).

When the liquid composition given by Eq. [4] intersects a monovariant eutectic line, the remaining fraction liquid transforms to a binary-type eutectic and possibly the ternary eutectic (if the liquid composition is enriched to the ternary eutectic composition, as discussed in Section II-A-2). Thus, the value of f_L at the intersection point of the primary solidification path and monovariant eutectic line defines the total amount of eutectic, f_e^t , in the microstructure. In order to determine the location of this intersection point on the monovariant eutectic line, the eutectic line is first represented by a linear equation:

$$C_{LA} = a + bC_{LB} \quad [5]$$

Polynomial and other types of expressions can be used to represent eutectic lines that exhibit curvature, but only the linear case will be considered here. Equating expressions [4] and [5] defines the unique value of B concentration in the liquid, C_{LB}^* , at the intersection point of the primary solidification path and monovariant eutectic line.

$$a + bC_{LB} = \frac{C_{oA}}{\left(\frac{1 - k_{\alpha A}}{1 - k_{\alpha B}}\right) \left(\frac{C_{oB} - k_{\alpha B} C_{LB}}{C_{LB}}\right) + k_{\alpha A}} \quad [6]$$

Equation [6] is solved for C_{LB}^* with a numerical technique and the corresponding value of total eutectic is then given by back-substitution of this value into Eq. [3b]

$$f_e^t = \frac{C_{oB} - k_{\alpha B} C_{LB}^*}{(1 - k_{\alpha B}) C_{LB}^*} \quad [7]$$

The corresponding value of primary α solid, f_α^p , is then given simply by

$$f_\alpha^p = 1 - f_e^t \quad [8]$$

2. Monovariant $L \rightarrow (\alpha + \beta)$ solidification

When the primary solidification path intersects a monovariant eutectic line, the $L \rightarrow \alpha$ reaction is replaced by either the $L \rightarrow (\alpha + \beta)$ or $L \rightarrow (\alpha + \gamma)$ reaction, and the mass balance expressions have to include formation of the new solid phase (either β or γ). Taking the $L \rightarrow (\alpha + \beta)$ as an example, the simple mass balance for each solute element is

$$C_{oA} = f_L C_{LA} + f_\alpha C_{\alpha A} + f_\beta C_{\beta A} \quad [9a]$$

$$C_{oB} = f_L C_{LB} + f_\alpha C_{\alpha B} + f_\beta C_{\beta B} \quad [9b]$$

The previous expressions are written assuming that the primary $L \rightarrow \alpha$ reaction is followed by the monovariant $L \rightarrow$

$(\alpha + \beta)$ reaction. If the $L \rightarrow (\alpha + \gamma)$ reaction occurs instead, then the $f_\beta C_{\beta A}$ and $f_\beta C_{\beta B}$ terms are replaced by $f_\gamma C_{\gamma A}$ and $f_\gamma C_{\gamma B}$, respectively. The solid and liquid compositions for each element in each phase are related by the equilibrium distribution coefficients.

For element A,

$$C_{\alpha A} = k_{\alpha A} C_{LA} \quad [10a]$$

$$C_{\beta A} = k_{\beta A} C_{LA} \quad [10b]$$

For element B,

$$C_{\alpha B} = k_{\alpha B} C_{LB} \quad [11a]$$

$$C_{\beta B} = k_{\beta B} C_{LB} \quad [11b]$$

From simple conservation of mass,

$$f_\beta = 1 - f_L - f_\alpha \quad [12]$$

Equations [9] through [12] can be combined to obtain a unique solution for f_L in terms of the nominal alloy composition, distribution coefficients, and composition of liquid along the monovariant eutectic line. The final expression is

$$f_L = \frac{\left(\frac{C_{oB} - k_{\beta B} C_{LB}}{C_{LB}(k_{\alpha B} - k_{\beta B})}\right) - \left(\frac{C_{oA} - k_{\beta A} C_{LA}}{C_{LA}(k_{\alpha A} - k_{\beta A})}\right)}{\left(\frac{1 - k_{\beta B}}{k_{\alpha B} - k_{\beta B}}\right) - \left(\frac{1 - k_{\beta A}}{k_{\alpha A} - k_{\beta A}}\right)} \quad [13]$$

Note that C_{LA} and C_{LB} are related along the monovariant eutectic line by Eq. [5]. The starting point for the liquid compositions for Eq. [13] are provided by the values of C_{LA}^* and C_{LB}^* (determined in Section II-A-1) that represent the intersection point of the primary solidification path and monovariant eutectic line. Equation [13] can be used to determine if the liquid composition becomes fully enriched in solute to the ternary eutectic $L \rightarrow (\alpha + \beta + \gamma)$ point and can therefore be used to determine the final weight fractions of binary α/β ($f_{\alpha/\beta}$) and ternary $\alpha/\beta/\gamma$ eutectic ($f_{\alpha/\beta/\gamma}$) constituents. Two possibilities exist. If all of the liquid is consumed along the monovariant eutectic line before the ternary eutectic reaction is reached, then $f_{\alpha/\beta} = f_e^t$, where f_e^t is determined from Eq. [7]. If the liquid is enriched to the ternary eutectic composition, then $f_{\alpha/\beta/\gamma}$ is given by the value of f_L from Eq. [13] at the ternary eutectic point and $f_{\alpha/\beta} = f_e^t - f_{\alpha/\beta/\gamma}$. Examples that demonstrate the use of these equations will be provided in Section III.

B. Paraequilibrium Solidification

The assumptions invoked for this condition are similar to equilibrium except that one solute now displays negligible diffusion in the solid phases. The expressions developed below assume infinite diffusion of element B in the solid phases and negligible diffusion of element A in the solid phases.

1. Primary $L \rightarrow \alpha$ solidification

The relation between fraction liquid and liquid composition for solute A is now given by the Scheil equation, whereas Eq. [3b] still holds for element B.

$$f_L = \left(\frac{C_{LA}}{C_{oA}} \right)^{\frac{1}{k_{\alpha A} - 1}} \quad [14a]$$

$$f_L = \frac{C_{oB} - k_{\alpha B} C_{LB}}{(1 - k_{\alpha B}) C_{LB}} \quad [14b]$$

Proceeding in the same manner used to obtain Eq. [4], the solidification path for this condition is given by

$$C_{LA} = C_{oA} \left(\frac{C_{oB} - k_{\alpha B} C_{LB}}{(1 - k_{\alpha B}) C_{LB}} \right)^{k_{\alpha A} - 1} \quad [15]$$

This expression is analogous to Eq. [4] and is used in a similar manner. The unique value of C_{LB}^* at the intersection point of the primary solidification path and monovariant eutectic line is given by

$$a + b C_{LB} = C_{oA} \left(\frac{C_{oB} - k_{\alpha B} C_{LB}}{(1 - k_{\alpha B}) C_{LB}} \right)^{k_{\alpha A} - 1} \quad [16]$$

The value of C_{LB}^* given by Eq. [16] can be back-substituted into Eq. [7] to determine the value of f_e^t , and f_{α}^p is given by Eq. [8].

2. Monovariant $L \rightarrow (\alpha + \beta)$ solidification

The simple mass balance for element B is still valid along the monovariant eutectic line (Eq. [9b]) because the diffusion rate of B in the solid phases is still considered infinite, but a differential mass balance is needed for negligible diffusion of element A in the solid phases. The pertinent mass balance equations are

$$f_L dC_{LA} = df_{\alpha}(C_{LA} - C_{\alpha A}) + df_{\beta}(C_{LA} - C_{\beta A}) \quad [17a]$$

$$C_{oB} = f_L C_{LB} + f_{\alpha} C_{\alpha B} + f_{\beta} C_{\beta B} \quad [17b]$$

Conservation of mass is represented in differential form (by differentiating Eq. [12]):

$$df_{\alpha} = -df_{\beta} - df_L \quad [18]$$

Inserting Eqs. [10] and [18] into Eq. [17a] and solving for df_L/dC_{LA} ,

$$\frac{df_L}{dC_{LA}} = \frac{f_L}{C_{LA}(k_{\alpha A} - 1)} - \left(\frac{k_{\alpha A} - k_{\beta A}}{k_{\alpha A} - 1} \right) \frac{df_{\beta}}{dC_{LA}} \quad [19]$$

Equation [19] describes the variation in fraction liquid along the monovariant eutectic line. The starting values of f_L and C_{LA} are determined by the intersection of the primary solidification path and monovariant eutectic line

and are therefore known. The df_{β}/dC_{LA} term can be determined from the mass balance for element B. Inserting Eqs. [11] and [12] into Eq. [17b] and solving for f_{β} ,

$$f_{\beta} = \frac{C_{oB} - C_{LB}[f_L(1 - k_{\alpha B}) + k_{\alpha B}]}{C_{LB}(k_{\beta B} - k_{\alpha B})} \quad [20]$$

The term df_{β}/dC_{LB} is then given by

$$\frac{df_{\beta}}{dC_{LB}} = \frac{C_{oB}}{(k_{\alpha B} - k_{\beta B}) C_{LB}^2} \quad [21]$$

The terms dC_{LA} and dC_{LB} along the monovariant eutectic line are related through Eq. [5]:

$$\frac{dC_{LA}}{dC_{LB}} = b \quad [22]$$

Combining Eqs. [19], [21], and [22],

$$\frac{df_L}{dC_{LA}} = \left(\frac{f_L}{C_{LA}(k_{\alpha A} - 1)} \right) - \left(\frac{k_{\alpha A} - k_{\beta A}}{k_{\alpha B} - k_{\beta B}} \right) \left(\frac{C_{oB}}{b(k_{\alpha A} - 1) C_{LB}^2} \right) \quad [23]$$

This expression is similar to Eq. [13], except that the variation in f_L along the monovariant eutectic line must be determined with an iterative technique. The initial value for df_L/dC_{LA} is determined by using the values of f_L , C_{LA} , and C_{LB} at the intersection point of the primary solidification path and monovariant eutectic line. The value of C_{LA} is then incremented a very small amount ΔC_{LA} along the monovariant eutectic line and the corresponding value of C_{LB} is determined through Eq. [5]. The new value of fraction liquid at this point (f_L^{n+1}) is then determined by

$$f_L^{n+1} = f_L^n + \left(\frac{df_L}{dC_{LA}} \right)_n \Delta C_{LA} \quad [24]$$

This process is continued until the liquid is completely consumed during the monovariant reaction or the ternary eutectic point is reached. If all the liquid is consumed along the monovariant eutectic line before the ternary eutectic reaction is reached, then $f_{\alpha/\beta} = f_e^t$. If the liquid is enriched to the ternary eutectic composition, then $f_{\alpha/\beta/\gamma}$ is given by the value of f_L at the ternary eutectic point and $f_{\alpha/\beta} = f_e^t - f_{\alpha/\beta/\gamma}$.

C. Nonequilibrium Solidification

This condition was originally developed by Mehrabian and Flemings^[6] and more recently summarized and applied to understand microstructural development in Ni-base superalloys.^[7] The treatment is briefly reviewed here. The assumptions invoked for this condition are similar to the conditions previously considered except that both solutes now display negligible diffusion in the solid phases.

1. Primary $L \rightarrow \alpha$ solidification

The Scheil expression provides the relation between fraction liquid and liquid composition for each element:

$$f_L = \left(\frac{C_{LA}}{C_{oA}} \right)^{\frac{1}{k_{\alpha A} - 1}} \quad [25a]$$

$$f_L = \left(\frac{C_{LB}}{C_{oB}} \right)^{\frac{1}{k_{\alpha B} - 1}} \quad [25b]$$

The corresponding solidification path is given by

$$C_{LA} = C_{oA} \left(\frac{C_{LB}}{C_{oB}} \right)^{\frac{k_{\alpha A} - 1}{k_{\alpha B} - 1}} \quad [26]$$

The unique value of C_{LB}^* at the intersection point is then given as

$$a + bC_{LB} = C_{oA} \left(\frac{C_{LB}}{C_{oB}} \right)^{\frac{k_{\alpha A} - 1}{k_{\alpha B} - 1}} \quad [27]$$

This unique value of C_{LB}^* is used with Eq. [25b] to determine f_e^t

$$f_e^t = \left(\frac{C_{LB}^*}{C_{oB}} \right)^{\frac{1}{k_{\alpha B} - 1}} \quad [28]$$

The fraction of primary phase is then given by Eq. [8].

2. Monovariant $L \rightarrow (\alpha + \beta)$ solidification

The differential mass balance for each element is given by (following Eq. [19])

$$\frac{df_L}{dC_{LA}} = \frac{f_L}{C_{LA}(k_{\alpha A} - 1)} - \left(\frac{k_{\alpha A} - k_{\beta A}}{k_{\alpha A} - 1} \right) \frac{df_{\beta}}{dC_{LA}} \quad [29a]$$

$$\frac{df_L}{dC_{LB}} = \frac{f_L}{C_{LB}(k_{\alpha B} - 1)} - \left(\frac{k_{\alpha B} - k_{\beta B}}{k_{\alpha B} - 1} \right) \frac{df_{\beta}}{dC_{LB}} \quad [29b]$$

Solving Eq. [29b] for df_{β}/dC_{LB} and combining this with Eq. [22] leads to an expression for df_{β}/dC_{LA}

$$\frac{df_{\beta}}{dC_{LA}} = \left(\frac{f_L}{k_{\alpha B} - k_{\beta B}} \right) \left(\frac{1}{bC_{LB}} \right) - \left(\frac{k_{\alpha B} - 1}{k_{\alpha B} - k_{\beta B}} \right) \frac{df_L}{dC_{LA}} \quad [30]$$

Combining Eqs. [29a] and [30] provides the final expression for df_L/dC_{LA} :

$$\frac{df_L}{dC_{LA}} = \left(\frac{\left(\frac{f_L}{k_{\alpha A} - 1} \right) \left[\frac{1}{C_{LA}} - \left(\frac{k_{\alpha A} - k_{\beta A}}{k_{\alpha B} - k_{\beta B}} \right) \left(\frac{1}{bC_{LB}} \right) \right]}{\left[1 - \left(\frac{k_{\alpha A} - k_{\beta A}}{k_{\alpha B} - k_{\beta B}} \right) \left(\frac{k_{\alpha B} - 1}{k_{\alpha A} - 1} \right) \right]} \right) \quad [31]$$

Equation [31] is analogous to Eq. [23] and is used in the same manner. This condition of ternary nonequilibrium solidification is similar to the binary case in that the liquid composition will always become enriched to a local invariant point on the liquidus surface, *i.e.*, the ternary eutectic point. Thus, some finite amount of terminal eutectic will

always form. This value of $f_{\alpha/\beta/\gamma}$ is given by the value of f_L at the ternary eutectic point, and $f_{\alpha/\beta} = f_e^t - f_{\alpha/\beta/\gamma}$.

III. EXAMPLE APPLICATIONS OF SOLUTE REDISTRIBUTION EQUATIONS

Figure 4 shows the C-rich corner of a hypothetical A-B-C ternary eutectic system that will be used to demonstrate the range of solidification behavior that can form under the three conditions considered here. As with the previous sections, the results for the paraequilibrium condition are shown for the case for infinite diffusion of element B in the solid phases and negligible diffusion of element A in the solid phases. Factors that affect the primary solidification path will be discussed first.

A. Primary Solidification Paths

Figure 5 shows the primary solidification paths for an alloy in which the nominal concentration of A and B and distribution coefficients for each element in primary α are equivalent ($C_{oA} = C_{oB} = 5$ wt pct and $k_{\alpha A} = k_{\alpha B} = 0.5$). Thus, the only factor that affects the primary solidification paths is the diffusion behavior of solutes in the solid phases. The equilibrium and nonequilibrium cases coincide, while the solidification path for the paraequilibrium case is always richer in element A. Solidification terminates before any monovariant eutectic line is reached for the equilibrium case (the location of termination is noted for the equilibrium case in Figure 5), while the primary solidification path always reaches a eutectic line for the nonequilibrium case (the nonequilibrium case coincidentally intersects the ternary eutectic point in Figure 5). The similarity in solidification paths for the equilibrium and nonequilibrium case occurs because each solute partitions between the liquid and solid phases in the same manner, *i.e.*, each element diffuses either infinitely fast or not at all in the solid phase, and the degree of partitioning between the liquid and the solid is identical (because the k values for each element are identical).

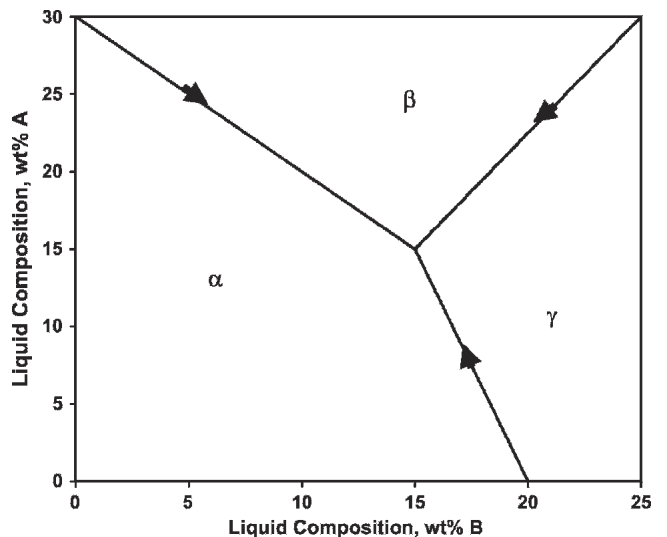


Fig. 4—Hypothetical ternary eutectic system used for example calculations.

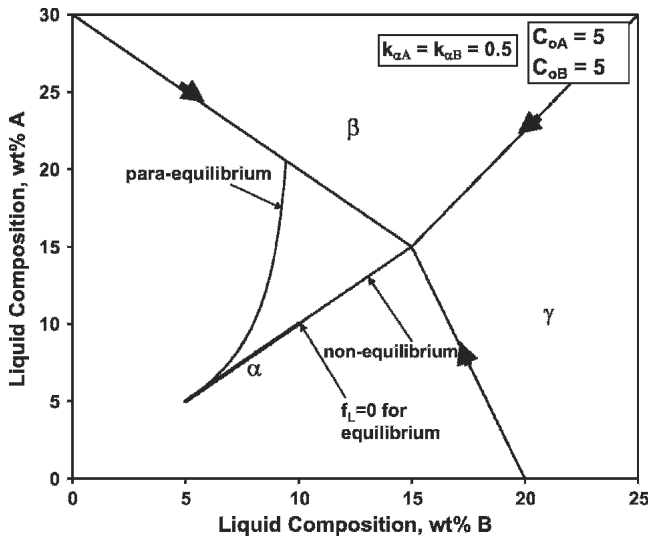


Fig. 5—Calculated primary solidification paths for an alloy with $C_{oA} = C_{oB} = 5$ wt pct and $k_{\alpha A} = k_{\alpha B} = 0.5$.

The differences between equilibrium and nonequilibrium results lie within the termination point. Note from Eq. [3] that the maximum solute enrichment in the liquid for the equilibrium case occurs when $C_{Li} = C_{oi}/k_{\alpha i}$, at which point $f_L = 0$ and solidification is complete. If this maximum value is reached before the intersection point, then no eutectic will form. This is equivalent to stating that the nominal alloy composition is less than the maximum solid solubility. However, for the nonequilibrium case, $C_{Li} \rightarrow \infty$ as $f_L \rightarrow 0$ (Eq. [25]), which indicates that the eutectic reaction will always be reached. This occurs for nonequilibrium solidification because the primary solid does not dissolve all of the solute in the alloy due to incomplete diffusion. The paraequilibrium case is always more highly enriched in element A because that element does not diffuse in the primary solid. The inability of a particular element to diffuse in the primary solid causes less of that element to be incorporated into the solid, resulting in more solute enrichment in the liquid. As shown in Figure 5, this has a significant effect on the primary solidification path. Finally, also note from Eq. [14a] that $C_{LA} \rightarrow \infty$ as $f_L \rightarrow 0$, so, like the nonequilibrium case, the paraequilibrium case will always be enriched to a monovariant eutectic reaction.

Figure 6 shows similar results, except that the nominal alloy composition is different ($C_{oA} = 10$ wt pct, $C_{oB} = 5$ wt pct). The relative locations of the solidification paths are similar, but there are two main differences. First, the maximum possible solute enrichment in the liquid for the equilibrium case is greater than the intersection point, so the $L \rightarrow (\alpha + \beta)$ reaction is reached. Second, the slopes of the solidification paths are higher because $C_{oA} > C_{oB}$.

Figure 7 shows conditions identical to that of Figure 5, except that $k_{\alpha A}$ has been reduced from 0.5 to 0.2, so that element A now segregates more strongly to the liquid than element B. The reduction in $k_{\alpha A}$ causes all of the curves to shift up due to the increased segregation of element A. This has the influence of favoring the $L \rightarrow (\alpha + \beta)$ reaction over the $L \rightarrow (\alpha + \gamma)$ reaction. In addition, the equilibrium and nonequilibrium solidification paths no longer coincide.

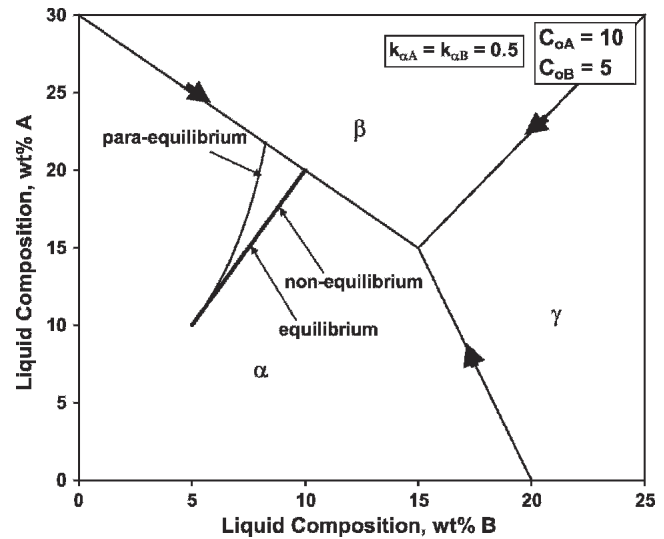


Fig. 6—Calculated primary solidification paths for an alloy with $C_{oA} = 10$ wt pct, $C_{oB} = 5$ wt pct, and $k_{\alpha A} = k_{\alpha B} = 0.5$.

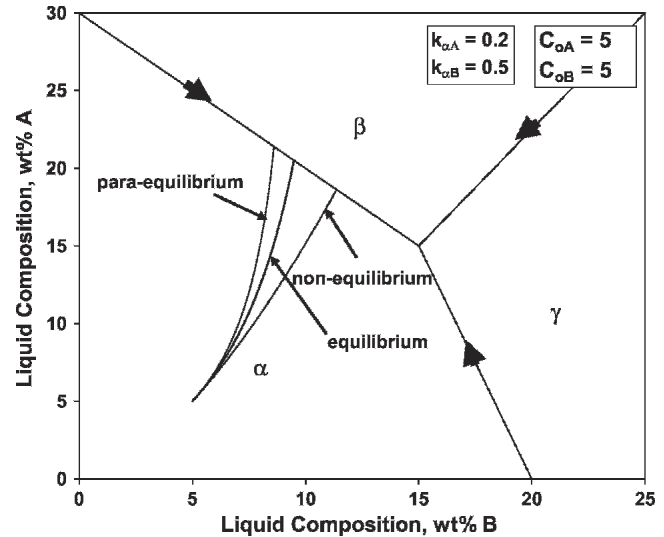


Fig. 7—Calculated primary solidification paths for an alloy with $C_{oA} = C_{oB} = 5$ wt pct, $k_{\alpha A} = 0.2$, and $k_{\alpha B} = 0.5$.

The equilibrium path is above the nonequilibrium path due to the reduced $k_{\alpha A}$ value.

B. Combined Primary and Eutectic Solidification Results

This section summarizes the combined results of primary and eutectic solidification on the hypothetical ternary system. Table I summarizes the values of equilibrium distribution coefficients and parameters for the linear equations that represent the α/β and α/γ eutectic lines. The ternary eutectic point occurs at $C_{LA} = 15$ wt pct A and $C_{LB} = 15$ wt pct B. The β phase is assumed to be A rich and the γ phase is assumed to be B rich. This is reflected in the $k_{\beta A}$ and $k_{\gamma B}$ values that are greater than unity. Table II summarizes the composition of five different alloys that were modeled. The primary solidification paths for each alloy and condition are shown in Figures 8 through 11, and the calculated weight

Table I. Summary of Equilibrium Distribution Coefficients and Parameters for the Linear Equation That Represents the α/β and α/γ Eutectic Lines for Example Calculations

$k_{\alpha A} = 0.5$	$k_{\alpha B} = 0.7$	α/β eutectic line: $C_{LA} = 30 - C_{LB}$
$k_{\beta A} = 1.6$	$k_{\beta B} = 0.6$	α/γ eutectic line: $C_{LA} = 60 - C_{LB}$
$k_{\gamma A} = 0.8$	$k_{\gamma B} = 3.0$	

Table II. Composition of Alloys Used in Model Calculations

Alloy	C_{oA} , Wt Pct A	C_{oB} , Wt Pct B
1	10	5
2	5	10
3	5	15
4	10	15
5	3	19

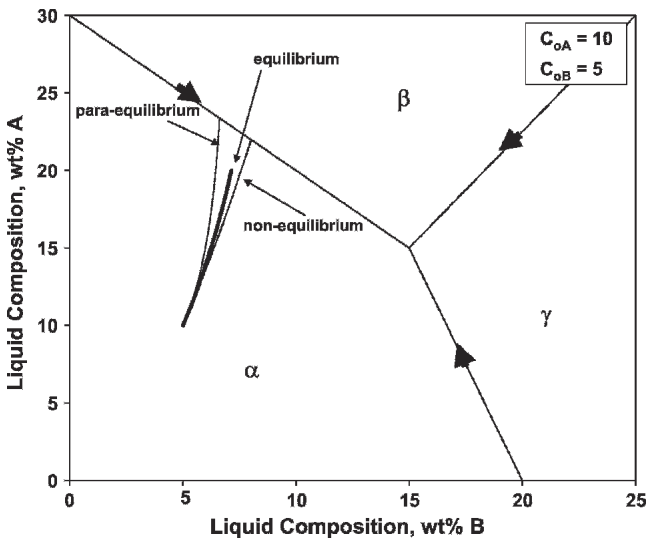


Fig. 8—Calculated primary solidification paths for an alloy with $C_{oA} = 10$ wt pct A, $C_{oB} = 5$ wt pct B and other parameters summarized in Table I.

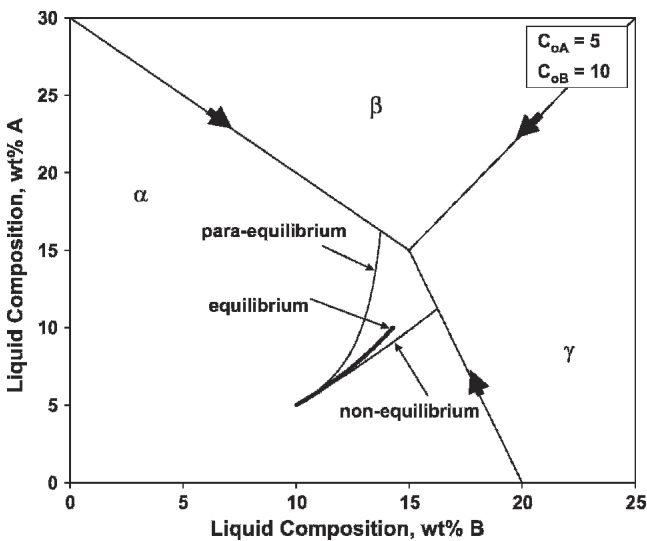


Fig. 9—Calculated primary solidification paths for an alloy with $C_{oA} = 5$ wt pct A, $C_{oB} = 10$ wt pct B and other parameters summarized in Table I.

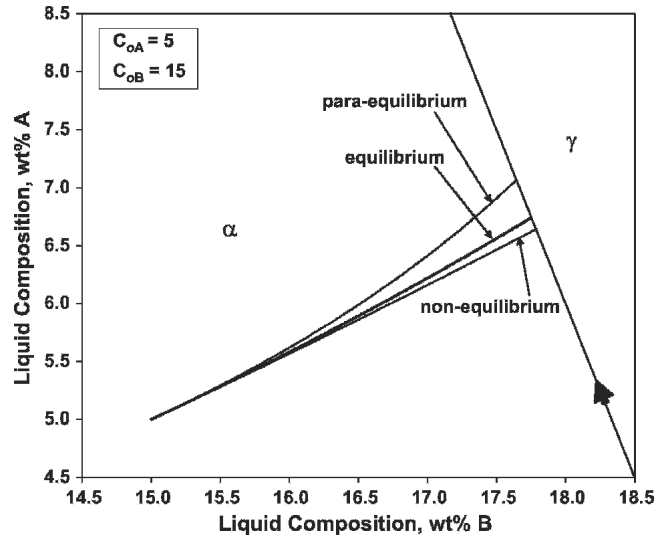


Fig. 10—Calculated primary solidification paths for an alloy with $C_{oA} = 5$ wt pct A, $C_{oB} = 15$ wt pct B and other parameters summarized in Table I.

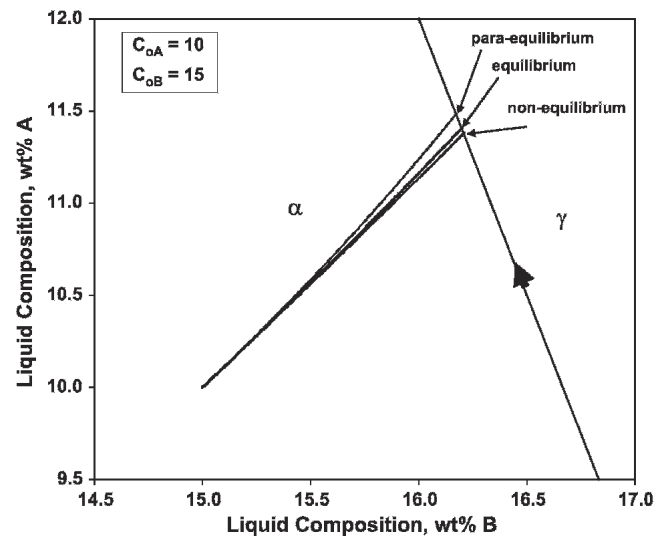


Fig. 11—Calculated primary solidification paths for an alloy with $C_{oA} = 10$ wt pct A, $C_{oB} = 15$ wt pct B and other parameters summarized in Table I.

fractions of the primary, monovariant, and ternary eutectic constituent for each alloy and condition are summarized in Figure 12. The nominal composition of alloy 5 lies directly on the α/γ eutectic line, so this alloy does not exhibit a primary $L \rightarrow \alpha$ stage of solidification.

These examples illustrate the rather wide range of results that can occur from the different solidification conditions. For the primary solidification path of alloy 1 under equilibrium conditions (Figure 8), the liquid composition is never enriched to the $L \rightarrow (\alpha + \beta)$ reaction and therefore the alloy only exhibits primary α after solidification. In contrast, the nonequilibrium case is enriched to the $L \rightarrow (\alpha + \beta)$ reaction and also proceeds to the terminal eutectic $L \rightarrow (\alpha + \beta + \gamma)$ point, so that the final microstructure contains 0.79 weight fraction primary α , 0.16 weight fraction of the binary-type α/β eutectic, and 0.05 weight fraction ternary

$\alpha/\beta/\gamma$ eutectic ($f_{\alpha}^p = 0.79$, $f_{\alpha/\beta} = 0.16$, and $f_{\alpha/\beta/\gamma} = 0.05$). For the paraequilibrium case, the primary solidification path intersects the $L \rightarrow (\alpha + \beta)$ reaction line, but the liquid is consumed during this reaction and the ternary eutectic constituent therefore does not form so that $f_{\alpha}^p = 0.81$, $f_{\alpha/\beta} = 0.19$, and $f_{\alpha/\beta/\gamma} = 0$.

Figure 9 shows the primary solidification paths for alloy 2 in which the position of the nominal alloy composition causes the nonequilibrium and paraequilibrium primary solidification paths to straddle the ternary eutectic point so that different monovariant eutectic reactions occur. Three significantly different results are obtained for each condition. As with the previous case, the equilibrium primary path does not reach a eutectic line so that $f_{\alpha}^p = 1$ and $f_{\alpha/\beta} = f_{\alpha/\beta/\gamma} = 0$. The paraequilibrium primary path intersects the $L \rightarrow (\alpha + \beta)$ reaction line, but the liquid is completely consumed along this line so that $f_{\alpha}^p = 0.91$, $f_{\alpha/\beta} = 0.09$, and $f_{\alpha/\beta/\gamma} = 0$. Finally, the nonequilibrium case intersects the $L \rightarrow (\alpha + \gamma)$ line so that the α/γ eutectic forms instead of the α/β eutectic, and the liquid composition is enriched to the ternary eutectic point with the final result of $f_{\alpha}^p = 0.8$, $f_{\alpha/\gamma} = 0.1$, and $f_{\alpha/\beta/\gamma} = 0.1$. Last, Figures 10 and 11 show the solidification paths for alloys 3 and 4 in which the nominal alloy composition is close to the α/γ eutectic reaction line. The final results for these two examples and alloy 5, which has a nominal composition located directly on the α/γ eutectic line, are summarized in Figure 12. These last examples generally show that less terminal ternary eutectic constituent is expected for the equilibrium case.

The results presented previously for ternary solidification show similarities to the companion binary cases. For example, a ternary eutectic alloy solidifying under equilibrium conditions will only exhibit the monovariant eutectic reaction when the nominal alloy concentration is above the maximum solid solubility. This result is similar to the binary case, in which the invariant $L \rightarrow (\alpha + \beta)$ eutectic reaction only occurs when the nominal composition is greater than the maximum solid solubility. For a ternary eutectic alloy solidifying under nonequilibrium conditions, the liquid is always enriched to a terminal invariant point so

that both the monovariant and invariant ternary eutectic reactions are always expected to occur. This case is similar to the binary nonequilibrium Scheil condition in which the liquid is always enriched to the invariant $L \rightarrow (\alpha + \beta)$ eutectic reaction, regardless of the nominal composition. The paraequilibrium condition lies between the equilibrium and nonequilibrium conditions in which a monovariant eutectic reaction is always expected to occur, but solidification can terminate before the invariant ternary eutectic reaction is reached.

IV. SELECTING A CONDITION

The difference among the three cases considered here is governed by the diffusivity of solutes in the solid phases. Thus, the condition that most closely describes the solidification behavior for an actual application can be assessed by considering factors that affect the ability of the solute to diffuse in the solid. This includes the inherent diffusivity of the solute, the solidification time (as controlled by the cooling rate and solidification temperature range), and the length of the concentration gradient (\sim half the dendrite spacing during dendritic growth). Brody and Flemings^[9] considered the influence of back-diffusion in the solid during solidification and showed that diffusion in the solid phase is insignificant when the dimensionless parameter $\alpha = (D_s t_f / L^2) \ll 1$, where D_s is the diffusivity of solute in the solid, t_f is the local solidification time, and L is half the dendrite spacing. Clyne and Kurz^[10] have shown that the Brody–Flemings model is only valid under limited solute diffusion when $\alpha < \sim 0.1$. The model breaks down at α values above this value, since, in the presence of a fast diffusing element, solute is no longer conserved within the volume element considered. Clyne and Kurz proposed an alternate form of the α parameter, although they recognized this alternate form is not based on a physical model. More recently, Kobayashi^[11] and Ohnaka^[12] have provided a more rigorous analysis of back-diffusion during solidification. These models can be used to assess the significance of solid-state diffusion during solidification and to select a condition that most closely represents the application of interest.

Recent results indicate that some general comments can be made in this regard for moderate cooling rate conditions typical of casting and arc welding (these general trends may not hold under higher cooling rate conditions typical of, for example, high energy density welding and splat quenching). It is well known that diffusion rates for interstitial elements in cubic crystal structures such as bcc and fcc are orders of magnitude higher than substitutional diffusion rates, and that substitutional diffusion rates in bcc are significantly higher than those in fcc. For example, it has been shown that solid-state diffusion can be assumed to occur infinitely fast during solidification for interstitial diffusion of carbon in bcc iron-based alloys^[10] and fcc nickel-based alloys.^[7] Significant substitutional solid-state diffusion can occur during primary solidification of bcc phases in ferritic Fe–Cr–Al alloys^[13] and stainless steels.^[14] In contrast, substitutional diffusion has generally been shown to be negligible during solidification of fcc iron-based^[13] and nickel-based alloys.^[7]

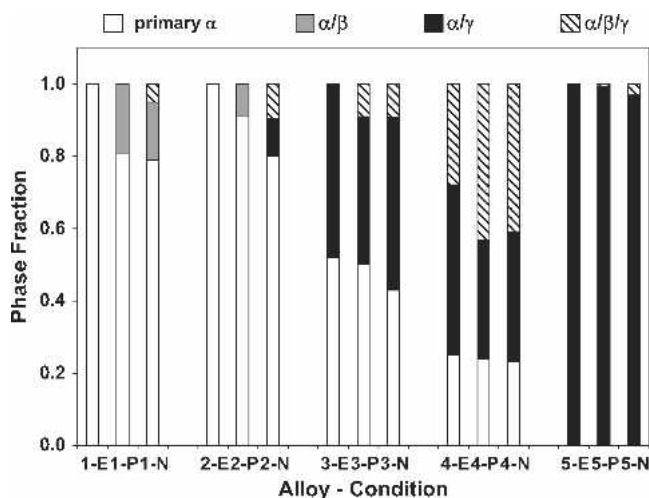


Fig. 12—Summary of phase fraction calculations for alloys listed in Table II. E—equilibrium condition, P—paraequilibrium condition, and N = nonequilibrium condition.

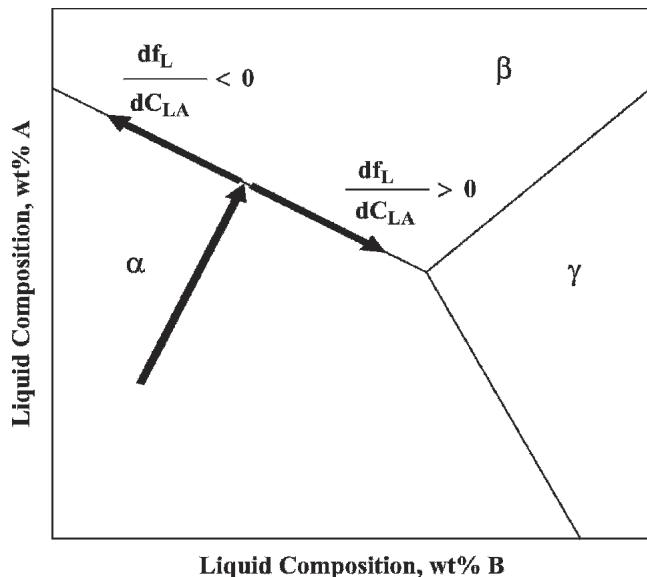


Fig. 13—Schematic illustration showing the relation between the sign of df_L/dC_{LA} and direction of decreasing temperature along the monovariant eutectic line.

V. DIRECTION OF EUTECTIC REACTIONS

In the examples, shown previously, a true ternary eutectic system was selected so that the minimum solidification temperature was associated with the invariant $L \rightarrow (\alpha + \beta + \gamma)$ reaction. In this case, the directions of decreasing temperature along the monovariant eutectic lines are known, and therefore, the direction of the solidification paths along these reactions are also known. However, systems exist in which the minimum solidification temperature associated with the terminal reaction can be located along a binary axis,^[7] so the direction of decreasing temperature and associated direction of the solidification path along a monovariant reaction line are not always known *a priori*. As shown schematically in Figure 13, the direction of the solidification path can be determined by the sign of df_L/dC_{LA} at the intersection of the primary solidification path and monovariant eutectic line. The signs of df_L/dC_{LA} for paraequilibrium and nonequilibrium are given by Eqs. [23] and [31], respectively. The equilibrium case can be determined by differentiating Eq. [13]. As expected, the sign of df_L/dC_{LA} is strongly influenced by the partitioning behavior of the solute elements between the solid phases as reflected in the relative values of k_{ij} .

VI. SUMMARY

A simple mathematical model has been developed for determining solidification paths in ternary alloys during the primary and monovariant stages of solidification for equilibrium, paraequilibrium, and nonequilibrium conditions. The results can be used to estimate the possible range of primary solidification paths, the type of monovariant reaction expected to occur, and the relative amount of pri-

mary, monovariant eutectic, and ternary eutectic constituents that form during solidification. Example calculations show that a range of solidification behavior can result from the three conditions considered. The direction of the solidification path along the monovariant eutectic line can also be determined from the sign of df_L/dC_{LA} and is affected by the partitioning behavior of solute elements between the solid phases.

ACKNOWLEDGMENTS

The author gratefully acknowledges financial support of this research from the National Science Foundation through Award No. DMI 0500254 and the Office of Naval Research through Contract No. N00014-06-1-0239. The author also acknowledges thoughtful review of the manuscript by Dr. W. Liu, Dr. M.J. Perricone, and Mr. T.D. Anderson.

NOMENCLATURE

C_{oj}	nominal concentration of element j
C_{Lj}	concentration of element j in liquid phase
$C_{i,j}$	concentration of element j in solid phase i
C_e	eutectic composition
C_{Lj}^*	concentration of element j in liquid at the intersection of primary solidification path and monovariant eutectic line
f_i	fraction of solid phase i
f_l	fraction of liquid phase
f_e	fraction eutectic
f_e^t	fraction of total eutectic
f_α^p	fraction of primary phase
$f_{\alpha/\beta}$	fraction of α/β binary-type eutectic constituent
$f_{\alpha/\beta/\gamma}$	fraction of $\alpha/\beta/\gamma$ ternary eutectic constituent
$k_{i,j}$	equilibrium distribution coefficient for element j between phase i and the liquid
a	intercept of liquidus line on the liquidus projection
b	slope of liquidus line on the liquidus projection

REFERENCES

1. W.J. Boettinger, S.R. Coriell, A.L. Greer, A. Karma, W. Kurz, M. Rappaz, and R. Trivedi: *Acta Mater.*, 2000, vol. 48, pp. 43-70.
2. R. Trivedi and W. Kurz: *Int. Mater. Rev.*, 1994, vol. 39, pp. 49-74.
3. V. Laxmanan: *Acta Mater.*, 1985, vol. 33, pp. 1023-35.
4. T.P. Battle: *Int. Mater. Rev.*, 1992, vol. 37, pp. 249-70.
5. E.Z. Scheil: *Metallkd.*, 1942, vol. 34, pp. 70-71.
6. R. Mehrabian and M.C. Flemings: *Metall. Trans.*, 1970, vol. 1, pp. 455-64.
7. J.N. DuPont, C.V. Robino, and A.R. Marder: *Acta Mater.*, 1998, vol. 46, pp. 4781-90.
8. M.J. Perricone, J.N. DuPont, and M.J. Cieslak: *Metall. Mater. Trans. A*, 2003, vol. 34A, pp. 1127-32.
9. H.D. Brody and M.C. Flemings: *Trans. AIME*, 1966, vol. 236, pp. 615-23.
10. T.W. Clyne and W. Kurz: *Metall. Trans. A*, 1981, vol. 12A, pp. 965-71.
11. S. Kobayashi: *J. Cryst. Growth*, 1988, vol. 88, pp. 87-94.
12. I. Ohnaka: *Trans. Iron Steel Inst.*, 1986, vol. 26, pp. 1045-51.
13. S.W. Banovic, J.N. DuPont, and A.R. Marder: *Welding J.*, 1999, vol. 78, pp. 23s-30s.
14. J.A. Brooks and A.W. Thompson: *Int. Mater. Rev.*, 1991, vol. 36, pp. 16-43.